

Layer-by-Layer Deposition of Rhenium-Containing Hyperbranched Polymers and Fabrication of Photovoltaic Cells

Chui Wan Tse,^[a] Ka Yan Kitty Man,^[a] Kai Wing Cheng,^[a] Chris S. K. Mak,^[a]
Wai Kin Chan,^{*[a]} Cho Tung Yip,^[b] Zheng Tong Liu,^[b] and Aleksandra B. Djurišić^[b]

Abstract: Multilayer thin films were prepared by the layer-by-layer (LBL) deposition method using a rhenium-containing hyperbranched polymer and poly[2-(3-thienyl)ethoxy-4-butylsulfonate] (PTEBS). The radii of gyration of the hyperbranched polymer in solutions with different salt concentrations were measured by laser light scattering. A significant decrease in molecular size was observed when sodium trifluoromethanesulfonate was used as the electrolyte. The conditions of preparing the multilayer thin films by LBL deposition were studied. The growth of the multilayer films was monitored by absorption spectroscopy and spectroscopic ellipsometry, and the surface mor-

phologies of the resulting films were studied by atomic force microscopy. When the pH of a PTEBS solution was kept at 6 and in the presence of salt, polymer films with maximum thickness were obtained. The multilayer films were also fabricated into photovoltaic cells and their photocurrent responses were measured upon irradiation with simulated air mass (AM) 1.5 solar light. The open-circuit voltage, short-circuit current, fill factor, and power conversion efficiency of the devices

were 1.2 V, 27.1 $\mu\text{A cm}^{-2}$, 0.19, and 6.1 $\times 10^{-3}\%$, respectively. The high open-circuit voltage was attributed to the difference in the HOMO level of the PTEBS donor and the LUMO level of the hyperbranched polymer acceptor. A plot of incident photon-to-electron conversion efficiency versus wavelength also suggests that the PTEBS/hyperbranched polymer junction is involved in the photosensitization process, in which a maximum was observed at approximately 420 nm. The relatively high capacitance, determined from the measured photocurrent rise and decay profiles, can be attributed to the presence of large counter anions in the polymer film.

Keywords: energy conversion • hyperbranched polymers • rhenium • self-assembly • thin films

Introduction

Polyelectrolyte multilayer deposition is a film-forming technique that involves the LBL deposition of two (or more) different polyelectrolytes with opposite charges. Since its development in the 1990s by Decher et al.,^[1,2] it has been widely used in the fabrication of different functional polymer thin films such as protein multilayers, sensors, ion transport membranes, capsules, and electro-optic materials.^[3] In addition, it can also be used to fabricate polymer–nanoparticle colloidal or polymer–ceramic composites when the surfa-

ces of the particles are decorated with charged functional groups.^[4–7] Compared to other conventional film-forming techniques, such as solution casting and spin-coating, this method enjoys the advantage that an ultrathin polymer film can be obtained with highly accurate control of thickness.^[8] Furthermore, the loss of materials during processing can also be kept to a minimum. More recently, this approach was used in the fabrication of polymer thin films for optoelectronic devices, such as field-effect transistors,^[9] light-emitting devices,^[10–15] and photovoltaic cells.^[16–19] A relatively low turn-on voltage was observed in the light-emitting diodes fabricated by multilayer deposition, which was attributed to the defect-free films obtained.^[10] Although the performances of these devices were not satisfactory compared to those of the extensively studied multilayer organic devices, the LBL deposition method provides an alternative approach to fabricate multilayer thin films. This is particularly important for the fabrication of thin films with complicated structures. In the LBL deposition process, only a single layer of polymer was deposited at a time. Therefore, it is possible

[a] C. W. Tse, K. Y. K. Man, K. W. Cheng, Dr. C. S. K. Mak, Dr. W. K. Chan
Department of Chemistry, The University of Hong Kong
Pokfulam Road, Hong Kong (China)
Fax: (+852) 2857-1586
E-mail: waichan@hku.hk

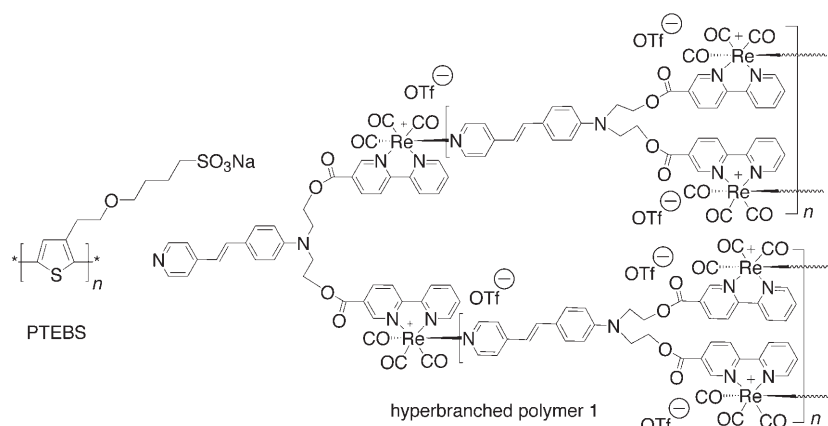
[b] C. T. Yip, Z. T. Liu, Dr. A. B. Djurišić
Department of Physics, The University of Hong Kong
Pokfulam Road, Hong Kong (China)

to prepare polymer blends composed of different functional polymers in the multilayer, which will be quite difficult to achieve by the conventional polymer film-forming methods.

We have been continuously developing metal-containing polymers in which the metal complex can play different roles, such as photosensitizers, charge carriers, and light emitters.^[20–23] Due to the fact that many of these polymers contain charged metal complexes, they are potential candidates for multilayer film formation using the LBL process. Recently, we have demonstrated the fabrication of photovoltaic cells using the LBL deposition method. A conjugated polymer functionalized with ruthenium terpyridine complex^[24] was codeposited with sulfonated polyaniline.^[25] The ruthenium complex can act as sensitizer in the photoinduced charge generation process. Here, we report the fabrication of multilayer thin films and their photosensitizing properties using a recently reported rhenium complex containing hyperbranched polymer.^[26] The polymer can self-assemble on a suitable substrate by electrostatic attraction. To the best of our knowledge, reports on the LBL assembly of dendrimers have been sparse, and most of the work reported is related to dendritic poly(amidoamine) derivatives^[27–31] or polyether.^[32] Herein, the hyperbranched polymer was codeposited with a charged polythiophene derivative that acted as the charge carrier. The effect of deposition conditions on the film properties was studied. In addition, photovoltaic cells were fabricated and the roles of these polymers in the photosensitization process were investigated.

Results and Discussion

Synthesis and characterization of polymers: The synthesis and characterization of hyperbranched polymer **1** (Scheme 1) was reported previously.^[26] It was synthesized by a one-step reaction in which the monomer units were linked together by coordination between the stilbazole ligand and the rhenium center. GPC analysis showed two peaks in the chromatogram, and the high-molecular-weight peak was attributed to the interaction between the charged polymer and the column materials.^[33] We further studied the effect of



Scheme 1. Structures of the polymers used in multilayer thin-film deposition. OTf = trifluoromethylsulfonate.

salt on the polymer molecular size by static light scattering. In pure DMF solution, the radius of gyration r_g of the polymer was measured as 23.5 nm. This value agrees with our previous atomic force microscopic (AFM) studies in which the size of the polymer molecules deposited on a silicon wafer was found to be 25–30 nm.^[26] Such a large molecular size may be due to the repulsion between charges on different branches in the polymer molecule, which lead to a more extended conformation. In general, r_g decreases with the concentration of salt in polyelectrolyte solution due to the screening of charges by the excess counterions added,^[34,35] and the presence of salt may also suppress the aggregation of polymer molecules.^[36] The r_g values of polymer **1** in the presence of different electrolytes were measured and the results are shown in Figure 1. In all cases, the r_g of the polymer decreases with increasing salt concentration. When

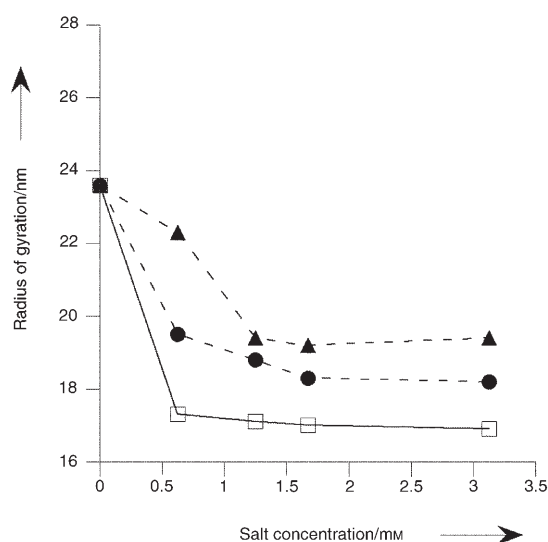


Figure 1. Plots of radii of gyration of polymer **1** (in DMF solution) in the presence of different salts. NaOTf □, NaPF₆ ●, Ba(OTf)₂ ▲.

NaOTf was used as the electrolyte, the most significant decrease in r_g was observed, which was measured as 16.9 nm. It was proposed that r_g decreased with salt concentration c_s proportionally by a power law $r_g \sim c_s^{-b}$, with exponent $b \sim 0.15–0.25$ for some common polyelectrolytes with linear molecular structure.^[35] In our case, such a correlation was not observed, which is probably due to the branched molecular structure in polymer **1**.

Formation of multilayer thin films:

The fabrication of polyelectrolyte multilayers is dependent on several different parameters, such as deposition time, solution concentration, pH, presence of other electrolytes, and solvent composi-

tion.^[3] In our work, the LBL deposition conditions for the formation of multilayers between PTEBS and polymer **1** were studied. PTEBS is a self-doped conducting polymer when in acidic form. The absorption spectrum may change according to the acidity of the solution.^[37–39] As polymer **1** is only soluble in DMF, the LBL deposition was carried out in DMF solution in conjunction with an aqueous solution of PTEBS. Accordingly, the rinsing steps were modified to prevent the abrupt change in solvent polarity and precipitation of **1** in water. After the deposition of polymer **1**, the substrate was rinsed with pure DMF, ethanol, and then water before it was dipped into aqueous PTEBS solution. Ethanol acted as the “transition solvent” between immersing the substrate in DMF and water. Table 1 summarizes the dip-

Table 1. Conditions used for the deposition of polymer **1**/PTEBS multilayer thin films; 80 bilayers were deposited for each sample. The concentrations of polymer **1** and PTEBS solutions were 0.09 and 0.17 mg mL⁻¹, respectively.

Entry	pH of PTEBS solution	NaOTf in polyelectrolyte ^[a]	Film thickness [nm] ^[b]	Roughness (rms) of film surface [nm] ^[c]
1	6	–	100	8
2	6	+	105	12
3	4.5	–	30	5
4	4.5	+	30	5

[a] When present, the concentration of NaOTf was kept at 10 mM. [b] Measured by step profiler. [c] Measured by AFM.

ping conditions used for the deposition of polymer **1**/PTEBS multilayer films. For comparison purposes, all the films were prepared by 80 deposition cycles. In all the experiments, the concentrations of PTEBS (in water) and polymer **1** (in DMF) were kept at 0.09 and 0.17 mg mL⁻¹, respectively. If the concentrations of PTEBS and polymer **1** were less than 0.04 and 0.1 mg mL⁻¹, respectively, very thin films (<5 nm) were obtained. The absorption spectrum of PTEBS solution is pH-dependent such that the absorption peak maximum shifted to a longer wavelength when the pH value was decreased.^[40] Multilayer thin films were fabricated from PTEBS solutions with different pH values. Thicker films were obtained when the multilayers were deposited at pH 6 compared to those obtained at pH 4.5 (Table 1, entries 1 and 3). One possible explanation is that at pH 4.5, PTEBS exists in a self-doped form^[37] in which the negative charges on the pendant sulfonate groups are partially balanced by the positive charges on the main chain, resulting in a reduction in charge density on the film surface.

The LBL deposition process is sensitive to the presence of electrolytes.^[41] The presence of salt in the solution may affect the “intrinsic” and “extrinsic” charge compensation on the film surface,^[42] which in turn affect the adsorption process and the morphology of the thin film obtained.^[43] The effect of addition of electrolyte on multilayer formation was studied. NaOTf (10 mM) was used in the studies to prevent other counterions from being introduced into the solutions. For the multilayers prepared at pH 6, the obtained

film thickness was found to increase slightly in the presence of salt (Table 1, entry 2), which might be due to the changes in polymer-chain conformation and molecular ions in solution. At a certain concentration, the polyelectrolytes take up an optimum conformation that may yield multilayer thin films with the largest thickness. For the film prepared at pH 4.5 (with or without salt added), no significant difference in film thickness was observed. This finding suggests that the pH of the PTEBS solution has a more significant effect on the resulting film thickness.

Figure 2a shows the changes in the absorption spectra of the polymer **1**/PTEBS multilayer thin film with different numbers of polymer layers deposited. The film was prepared according to the conditions listed in Table 1 (entry 3). When

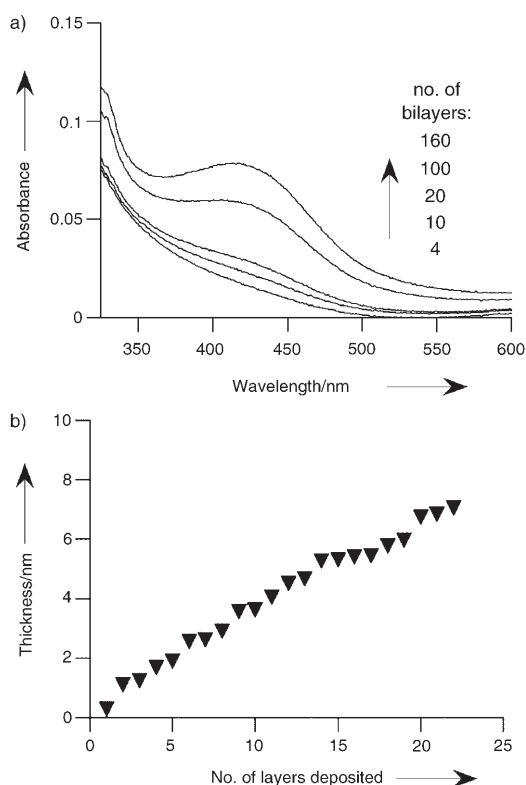


Figure 2. a) Absorption spectra of the polymer **1**/PTEBS multilayer film versus number of polymer layers deposited. b) Thickness of the polymer **1**/PTEBS multilayer measured by ellipsometry versus number of polymer layers. The multilayer film was prepared from a PTEBS solution of pH 4.5 in the absence of salt.

the number of polymer bilayers was gradually increased, an absorption band centered at about 420 nm started to appear. This is assigned to the metal-to-ligand charge transfer (MLCT) transition of the rhenium complex. With reference to the literature, PTEBS exhibits an absorption maximum at approximately 480 nm owing to the π - π^* transition in the conjugated main chain.^[40] However, this absorption peak only appeared as a shoulder when the number of bilayers was small. When the multilayer became thicker, the spectrum was dominated by the MLCT transition of the rhenium

complex. The presence of PTEBS in the multilayer is supported by the long absorption tail extending beyond 600 nm.

As the rate of increase in thickness for the films prepared at pH 4.5 is much slower compared to those obtained at pH 6, it is important to study the initial stage of the film deposition process in more detail. Spectroscopic ellipsometry was used to monitor the growth of the first few layers of polymer. Figure 2b shows the thickness of a polymer **1**/PTEBS multilayer film with up to 22 layers deposited (PTEBS solution, pH 4.5; no salt was added). The results suggest that the film thickness increased linearly over the thickness range studied. After 22 layers of polymer had been deposited, the thickness of the film was 7 nm, which is equivalent to a thickness increment of approximately 3 Å per layer. These data agree quite well with the results in Table 1 (entry 3). However, such an increment is obviously much smaller than the thickness of a monolayer of polymer molecules. One possible explanation is that the formation of a multilayer consists of many adsorptions and desorptions of polyelectrolytes,^[44] which results in a very slow increase in the multilayer film thickness.

Photovoltaic properties: In order to act as the active layer in photovoltaic devices, percolation pathways for the transport of holes and electrons must be established in the multilayer film. It should be noted that multilayers obtained by polyelectrolyte deposition do not exhibit distinct stratified layers. Instead, each layer of polymer molecules forms an interpenetrating network in which a polymer molecule may penetrate up to two to three layers of molecules above or below.^[8,45,46] The presence of such a network is essential to the transport of charges in the polymer film. The morphology of the multilayer film was studied by AFM. Figure 3 shows the AFM topographical and phase contrast images of polymer **1**/PTEBS with 80 bilayers (Table 1, entry 3). The root-mean-square (rms) roughness of the film was calculated to be 5 nm, and the roughness values of the multilayers prepared under different conditions are summarized in Table 1. The values of the rms roughness are quite similar to those of other reported polyelectrolyte multilayers.^[47] The topographical features observed in the height image are consistent with those in the phase image, indicating that the “peaks” and “valleys” observed correspond to materials of different nature. In addition, the interconnected domains in the phase-contrast image suggest that the surface of the polymer film consists of two components, which further supports the presence of an interpenetrating network.

Devices with the structure indium tin oxide (ITO)/(polymer **1**/PTEBS)₈₀/Al were fabricated by the LBL deposition process using the conditions listed in Table 1. It is envisaged that upon photoexcitation of the rhenium complex, excitons are formed and separated in the presence of an internal field. Holes will be transported via the PTEBS network while electrons will be transported via the rhenium-containing polymer. It was demonstrated previously that some polymeric rhenium complexes were able to act as both electron and hole carriers.^[48–50] The electrons were transported by

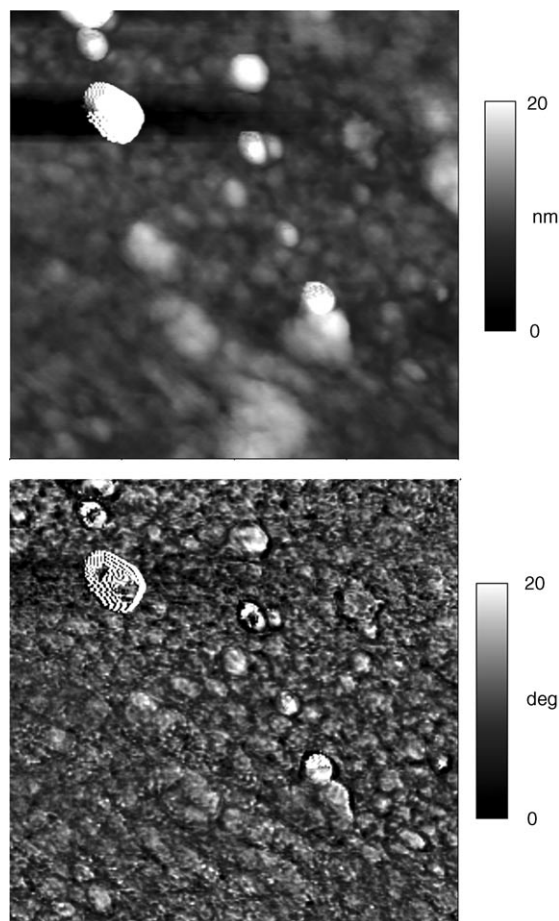


Figure 3. Topographical (top) and phase contrast (bottom) AFM images of polymer **1**/PTEBS multilayer (80 bilayers thick). The film was prepared from a PTEBS solution of pH 4.5 in the absence of salt. The scan sizes of both images are $1 \times 1 \mu\text{m}$.

hopping between the diimine ligands, which exhibited modest electron-carrier mobility. After evaporation of the aluminum electrode, the multilayered devices were irradiated with simulated AM 1.5 solar light. The current–voltage characteristics of the devices are summarized in Table 2. The typical current–voltage characteristics of devices 2 and 4 are shown in Figure 4. All the devices exhibit similar fill factors (FFs), and the power conversion efficiencies η_p are in the order of $10^{-3}\%$. It can be seen that those devices prepared from PTEBS solution with pH 6 exhibit the highest

Table 2. Photovoltaic properties of the devices ITO/(polymer **1**/PTEBS)₈₀/Al under illumination by AM 1.5 simulated solar light. The multilayer films were fabricated according to the conditions listed in Table 1.

Device ^[a]	I_{sc} [$\mu\text{A cm}^{-2}$]	V_{oc} [V]	FF	η_p [$10^{-3}\%$]	IPCE at 410 nm [%]
1	7.6	0.7	0.21	1.0	0.1
2	27.1	1.2	0.19	6.1	0.35
3	2	0.5	0.17	2.6	0.02
4	9.8	1.2	0.15	1.7	0.03

[a] Devices 1–4 were prepared according to the conditions described in Table 1 (entries 1–4).

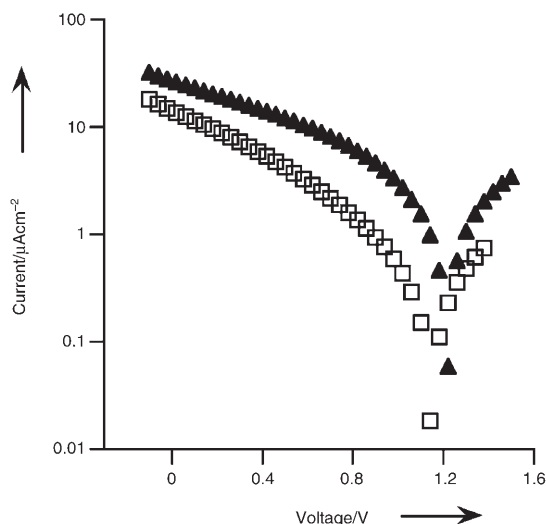


Figure 4. Current–voltage characteristics of photovoltaic devices comprising ITO/(polymer **1**/PTEBS)_n/Al (devices 2 ▲ and 4 □ in Table 2) under simulated AM 1.5 solar-light irradiation (100 mW cm^{-2}).

short-circuit current I_{sc} ($27.1 \mu\text{A cm}^{-2}$) and η_p ($6.1 \times 10^{-3}\%$). For those devices prepared from PTEBS solution with pH 4.5 (Table 2, devices 3 and 4), a relatively lower short-circuit current was obtained due to the small film thickness (low optical absorption). In addition, the bulk resistance of the multilayer films was in the order of 10^6 – $10^7 \Omega$, which may also contribute to the low short-circuit current. It should also be noted that the open-circuit voltage (V_{oc}) of device 2 is quite high (1.20 V), which is comparable to that of some heterojunction solar cells based on copper phthalocyanine and 3,4,9,10-perylene-tetracarboxylic bisbenzimidazole.^[51,52] The V_{oc} of an organic solar cell can be estimated from the difference between the HOMO of the electron donor and the LUMO of the acceptor. From the cyclic voltammogram of polymer **1**,^[53] the HOMO and LUMO levels of the polymer were estimated to be -5.6 and -3.6 V, respectively. The optical band gap observed in the edge of the absorption tail (Figure 2) also agrees with the HOMO–LUMO gap. From the literature, the HOMO and LUMO levels of PTEBS were -4.7 to -5.1 and -2.7 to -3.1 eV, respectively.^[54] Therefore, the difference between the HOMO of PTEBS and the LUMO of polymer **1** is 1.1 to 1.6 V, which agrees well with the observed V_{oc} values.

It is inferred that in these solar cells, PTEBS acts as the donor while polymer **1** acts as the electron acceptor. After the separation of excitons, holes were transported by the PTEBS network while electrons were transported by polymer **1**. The use of PTEBS as donor in polymer/TiO₂-type solar cells is known.^[54] A similar V_{oc} value (1.18 V) was also measured in device 4. However, devices 1 and 3, in which the multilayers were deposited in the absence of salt, exhibited much lower V_{oc} values (0.7 and 0.5 V, respectively). We suggest that the relatively poor performances of these devices may be due to several factors, which include charge recombination and low carrier mobility. The presence of salt

may also play a critical role in the exciton generation, separation, and charge transport processes. The relatively low fill factor may partly be due to low carrier mobility and inefficient contact between the polymer films and electrodes. However, such effects are not well understood and more examples of devices need to be fabricated. Incorporation of additional electron-carrying polyelectrolyte or a carefully chosen electrode contact may improve the device performance. It should be noted that the structures of these LBL films are quite similar to composites of inorganic nanoparticles/organic polymers. Recently, the use of such organic–inorganic nanocomposites was also employed in the fabrication of photovoltaic devices in which CdSe was codeposited with a poly(*p*-phenylenevinylene) derivative by the LBL process.^[55] In addition, the composites can be prepared by blending of ZnO^[56,57] or CuInS₂^[58] nanoparticles with conjugated polymers. Compared to these devices, the power conversion efficiencies of our cells are 1–2 orders of magnitude lower, which may be due to the lower charge-carrier mobilities.

The performances of photovoltaic cells in ambient atmosphere under continuous illumination of light were studied. After the multilayer polymer films were prepared, they were heated at 100°C in a vacuum oven for 24 h to remove the solvent residue. Figure 5 shows the change in short-cir-

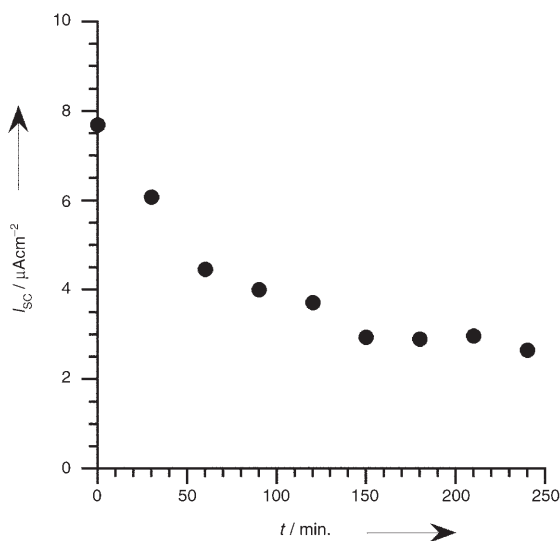


Figure 5. Plot of short-circuit current as a function of time for device 1 upon continuous illumination by simulated solar light (100 mW cm^{-2}). The experiment was carried out at 25°C under a relative humidity of 80%.

cuit current of device 1 upon illumination by simulated solar light (100 mW cm^{-2}) at 25°C and under a relative humidity of 80%. It can be seen that the current decreases to approximately 40% of the original value after 6 h. However, when the film was dried at 50°C in a vacuum oven, the current dropped to 10% of the original value. This finding clearly indicates the importance of the removal of water/solvent residue from the film in the device fabrication process.

Figure 6 shows the incident photon-to-electron conversion efficiency (IPCE) of device 2 at different wavelengths under the bias of 0, -0.5, and -1 V. The absorption spectrum of the multilayer film is also shown for comparison. It can

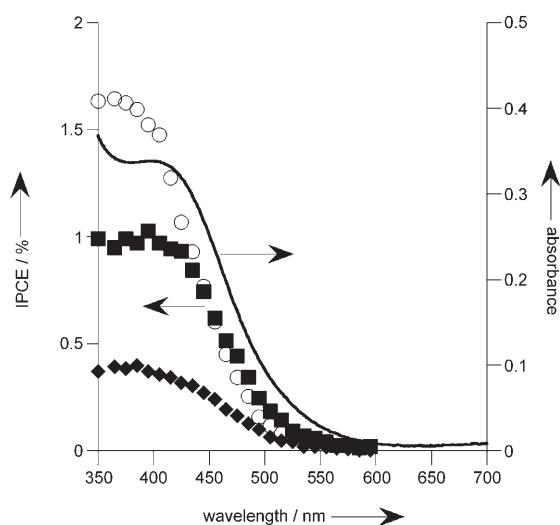


Figure 6. Plots of absorbance and incident photon-to-electron conversion efficiency (IPCE) of device 2 at different wavelengths under a bias of 0 (◆), -0.5 (■), and -1.0 V (○).

clearly be seen that the photocurrent response agrees very well with the absorption spectrum in which a local maximum is observed at about 430 nm. The IPCE values are comparable to those of other fullerene-based multilayer photovoltaic cells.^[59,60] In addition, the IPCE response extends to 600 nm. This indicates that the photosensitization process originates from the polymer 1/PTEBS junction that both polymers took part in during the photoinduced charge generation process. When a reverse bias was applied to the device, a significant increase in IPCE was observed. Therefore, the device may also serve as a photodetector with a selective sensitization range.

The charge transport behaviors of polymeric photovoltaic devices fabricated by the LBL process have been reported in the literature. The multilayers were mainly based on fullerene derivatives as the electron acceptors.^[59-63] It has been shown previously that the photocurrent generation and decay in polymer multilayers composed of poly(phenylene-vinylene), poly(acrylic acid), poly(allylamine hydrochloride), and fullerene can be fitted to a biexponential function. The multilayer films were regarded as a capacitor in which the charging process corresponds to the photoinduced electron-transfer process. In our system, the polymer multilayer was composed of a blend of a hyperbranched metal-containing polymer and an ionic PTEBS. Not only is the morphology of the polymer film different, but also the trifluoromethanesulfonate counterions present in the polymer films are relatively larger in size when compared to the other examples in the literature. Therefore, it is of fundamental interest to study the photoinduced charge generation and decay pro-

cesses by analyzing the photocurrent profile upon irradiation by light. Figure 7a shows the photocurrent profile when the device was irradiated with monochromatic light (400 nm with intensity $80 \mu\text{W cm}^{-2}$). Both the rise and decay of the transient photocurrent were simulated with multiple expo-

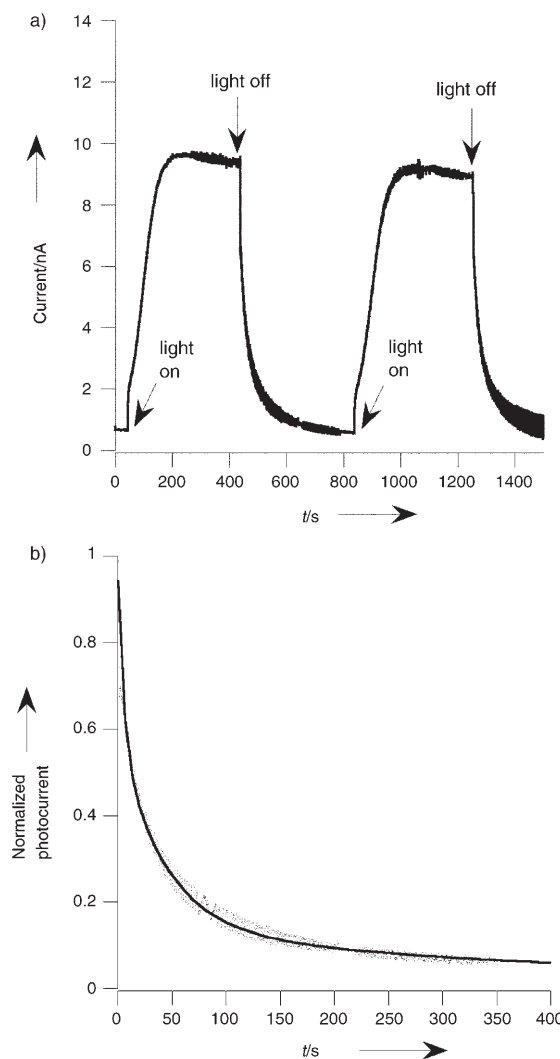


Figure 7. a) Photocurrent response as a function of time upon periodic illumination of device 2 with monochromatic light (400 nm with an intensity of $80 \mu\text{W cm}^{-2}$). b) Experimental photocurrent decay and the decay simulated using a triexponential function. Photocurrent simulated function —.

ponential functions, which could not be fitted into a biexponential function as proposed in the literature.^[64] However, good agreement with the experimental data was obtained when an additional exponential term was added, and the photocurrent decay can be described by Equation (1):

$$I(t) = I_1 \exp(-t/\tau_1) + I_2 \exp(-t/\tau_2) + I_3 \exp(-t/\tau_{\text{off}}) \quad (1)$$

The fitting result for the photocurrent decay is shown in Figure 7b. The values of I_1 , τ_1 , I_2 , τ_2 , and I_3 for the best-fitted curve were 0.38, 5.5 s, 0.45, 42.4 s, and 0.13, respective-

ly, while τ_{off} corresponds to the shutter off time (400 s). From these results, it is clear that two processes with time constants of approximately 5 and 40 s contribute almost equally to the decay of the photocurrent, which is different from the literature results in which the decay was dominated by τ_{off} . We suggest that the first term corresponds to the disappearance of free carrier in the polymers, and the second term corresponds to the redistribution of free ions in the polymer films. If the device is considered to be a capacitor in series with a resistor, from the time constant of the second exponential term and the resistance of the film (30 M Ω), the capacitance of the film was calculated to be 0.16 μF . This value is considerably greater than those of other polyelectrolyte multilayers reported previously (in the order of nanofarads).^[64,65] Similar fitting results were also obtained for the photocurrent rise profile. We attribute this finding to the relatively large anions present in the film when compared to other multilayers in which chloride ions were present. In addition, the morphology of the hyperbranched polymer may also affect the mobility of ions and generation of charge in the polymer films. At the moment, this phenomenon is not fully understood, and it constitutes a very interesting topic for further study in the future. It has previously been shown that charge transport in some metal complexes or metal-containing polymers^[66,67] is dependent on the electrolyte anion in the film. In addition, redox processes undertaken in the film may induce morphological changes.^[68] It should be noted that capacitances of the order of microfarads are observed in both liquid^[69] and solid-state^[70] dye-sensitized solar cells. Thus, techniques, such as impedance spectroscopic analysis, which are commonly used to investigate electronic and ionic processes in dye-sensitized solar cells, may also be useful for studying the charge transport in polyelectrolyte multilayers with mobile ions.

Conclusion

Multilayer thin films were fabricated from a metal-based hyperbranched polymer with an ionic PTEBS by the LBL deposition process. The effects of deposition conditions on the film properties were investigated and the photovoltaic properties of the devices fabricated from these multilayers were measured. The photocurrent responses of the devices suggest that the hyperbranched polymer/PTEBS junction participated in the photosensitization process. The studies of photocurrent rise and decay profiles suggest that the generation of photocurrent was affected by both the generation of free carriers and the presence of counterions in the multilayer film. Although the device efficiencies were relatively low, this deposition method provides a simple and versatile approach to fabricate photovoltaic cells by a solution method. There are many different issues that need to be understood in order to design a better device. For example, the effects of the presence of salt on the charge-carrier mobility require much more detailed studies. Moreover, the choice of electrodes, post-film-forming treatments (and hence film mor-

phology), and addition of further components may all affect the device performance. These will be very interesting research topics in the future and some of the work is in progress.

Experimental Section

Materials: All the reagents were purchased from Aldrich Chemicals or Lancaster Synthesis and were used as received. Hyperbranched polymer **1** was synthesized according to a previously published procedure.^[26] Sodium poly[2-(3-thienyl)ethoxy-4-butylsulfonate] (PTEBS) was purchased from American Dye Source. Ultrapure water (18.2 M Ω) was used in the preparation of polymer solutions and in the rinsing of all substrates/polymer films.

Instruments: UV/Vis spectra were collected on a Varian Cary 50 UV/Vis spectrometer. Atomic force micrographs were collected on a Digital Nanoscope IIIA scanning probe microscope. Static light scattering experiments were performed with a Wyatt Technology DAWN DSP laser photometer equipped with a He-Ne laser (632.8 nm). The ellipsometry data in the 700–800 nm spectral range were collected by using a J. A. Woollam V-VASE ellipsometer with 20-nm steps. The incidence angles were 65, 70, and 75°.

Multilayer thin film deposition: An ITO-coated glass slide (surface resistivity = 50 Ωsq^{-1}) was used as the substrate for the LBL deposition process. The substrate was cleaned by Decon 90, deionized water, acetone, methanol, methanol/toluene 1:1, and toluene in sequence. It was then immersed in a 3-aminopropyltrimethoxysilane solution (5% in toluene) for 12 h. The slide was rinsed with toluene, methanol/toluene 1:1, methanol, and deionized water in sequence. The deposition of one bilayer involved immersing the pretreated ITO-coated glass slide in the following solutions in sequence: water, PTEBS (0.09 mg mL^{-1} in H_2O), water, ethanol, DMF, polymer **1** in DMF (0.17 mg mL^{-1}), DMF, and ethanol. The dipping time for the two polyelectrolyte solutions was 15 min and the rinsing time for all other solvents was 2 min. The cycle was repeated until the desired number of bilayers was achieved. The growth process of the multilayer thin film was monitored by spectroscopic ellipsometry. The multilayer film was dried in a vacuum oven at 100°C for 24 h. Devices for photovoltaic measurements were fabricated by coating an aluminum electrode (40 nm) on the multilayer thin film under high vacuum. The photovoltaic properties of the multilayer thin films were studied by using simulated AM 1.5 solar light (Thermo Oriel 6255 150-W xenon lamp with an AM 1.5 filter) as the light source. Upon irradiation, the current–voltage characteristics of the device were measured with a Keithley 238 electrometer. The external quantum efficiency was determined by using the same light source with a Thermal Oriel Cornerstone 1/8 m monochromator for wavelength selection. The light intensity at each wavelength was measured with a Newport Optical Power Meter 1830-C.

Acknowledgements

This work was substantially supported by the Research Council of The Hong Kong Special Administrative Region (China, Project Nos. HKU 7096/02P, 7009/03P, 7008/04P, and 2/05C). Financial support from the Committee on Research and Conference Grant, University Development Fund, Outstanding Young Researcher Award, and The Seed Fund For Strategic Research Theme (University of Hong Kong) is also acknowledged.

- [1] G. Decher, J. D. Hong, *Makromol. Chem. Macromol. Symp.* **1991**, 46, 321.
- [2] G. Decher, J. D. Hong, J. Schmitt, *Thin Solid Films* **1992**, 210–211, 831.

- [3] G. Decher, J. B. Schlenoff, *Multilayer Thin Films: Sequential Assembly of Nanocomposite Materials*, Wiley-VCH, Weinheim, **2003**.
- [4] E. Hao, T. Lian, *Chem. Mater.* **2000**, *12*, 3392.
- [5] A. L. Rogach, D. S. Koktysh, M. Harrison, N. A. Kotov, *Chem. Mater.* **2000**, *12*, 1526.
- [6] D. W. Kim, A. Blumstein, S. K. Tripathy, J. Kumar, *Chem. Mater.* **2001**, *13*, 1916.
- [7] M. A. Correa-Duarte, A. Kosiorek, W. Kandulski, M. Giersig, L. M. Liz-Marzan, *Chem. Mater.* **2005**, *17*, 3268.
- [8] G. Decher, *Science* **1997**, *277*, 1232.
- [9] J. Locklin, K. Shinbo, K. Onishi, F. Kaneko, Z. Bao, R. C. Advincula, *Chem. Mater.* **2003**, *15*, 1404.
- [10] H. Hong, D. Davidov, Y. Avny, H. Chayet, E. Z. Faraggi, R. Neumann, *Adv. Mater.* **1995**, *7*, 846.
- [11] J. W. Baur, S. Kim, P. B. Balanda, J. R. Reynolds, M. F. Rubner, *Adv. Mater.* **1998**, *10*, 1452.
- [12] S. L. Clark, E. S. Handy, M. F. Rubner, P. T. Hammond, *Adv. Mater.* **1999**, *11*, 1031.
- [13] M. Eckle, G. Decher, *Nano Lett.* **2001**, *1*, 45.
- [14] A. C. Fou, O. Onitsuka, M. Ferreira, M. F. Rubner, B. R. Hsieh, *J. Appl. Phys.* **1996**, *79*, 7501.
- [15] J. Morgado, N. Barbagallo, A. Charas, L. Alcacer, *Synth. Met.* **2004**, *141*, 219.
- [16] J. W. Baur, M. F. Durstock, B. E. Taylor, R. J. Spry, S. Reulbach, L. Y. Chiang, *Synth. Met.* **2001**, *121*, 1547.
- [17] M. F. Durstock, B. Taylor, R. J. Spry, L. Chiang, S. Reulbach, K. Heitfeld, J. W. Baur, *Synth. Met.* **2001**, *116*, 373.
- [18] M. F. Durstock, R. J. Spry, J. W. Baur, B. E. Taylor, L. Y. Chiang, *J. Appl. Phys.* **2003**, *94*, 3253.
- [19] J. K. Mwaura, M. R. Pinto, D. Witker, N. Ananthkrishnan, K. S. Schanze, J. R. Reynolds, *Langmuir* **2005**, *21*, 10119.
- [20] S. C. Yu, X. Gong, W. K. Chan, *Macromolecules* **1998**, *31*, 5639.
- [21] W. Y. Ng, X. Gong, W. K. Chan, *Chem. Mater.* **1999**, *11*, 1165.
- [22] P. K. Ng, X. Gong, S. H. Chan, L. S. M. Lam, W. K. Chan, *Chem. Eur. J.* **2001**, *7*, 4358.
- [23] C. S. Hui, L. S. M. Lam, C. Yin, W. K. Chan, A. B. Djurišić, *J. Polym. Sci. Part A: Polym. Chem.* **2003**, *41*, 1708.
- [24] Z. Q. Lei, Y. P. Wang, *J. Appl. Polym. Sci.* **1997**, *64*, 1575.
- [25] K. Y. K. Man, H. L. Wong, W. K. Chan, C. Y. Kwong, A. B. Djurišić, *Chem. Mater.* **2004**, *16*, 365.
- [26] C. W. Tse, K. W. Cheng, W. K. Chan, A. B. Djurišić, *Macromol. Rapid Commun.* **2004**, *25*, 1335.
- [27] V. V. Tsukruk, F. Rinderspacher, V. N. Bliznyuk, *Langmuir* **1997**, *13*, 2171.
- [28] J. A. He, R. Valluzzi, K. Yang, T. Dolukhanyan, C. M. Sung, J. Kumar, S. K. Tripathy, L. Samuelson, L. Balogh, D. A. Tomalia, *Chem. Mater.* **1999**, *11*, 3268.
- [29] A. J. Khopade, F. Caruso, *Nano Lett.* **2002**, *2*, 415.
- [30] C. Li, K. Mitamura, T. Imae, *Macromolecules* **2003**, *36*, 9957.
- [31] B. Y. Kim, M. L. Bruening, *Langmuir* **2003**, *19*, 94.
- [32] F. W. Huo, H. P. Xu, L. Zhang, Y. Fu, Z. Q. Wang, X. Zhang, *Chem. Commun.* **2003**, 874.
- [33] M. A. Meier, B. G. G. Lohmeijer, U. S. Schubert, *Macromol. Rapid Commun.* **2003**, *24*, 852.
- [34] M. Sedlák, *Physical Chemistry of Polyelectrolytes* (Ed.: T. Radeva), Marcel Dekker, New York, **2001**, p. 1.
- [35] M. Beer, M. Schmidt, M. Muthukumar, *Macromolecules* **1997**, *30*, 8375.
- [36] M. Hara, J. Wu, A. H. Lee, *Macromolecules* **1989**, *22*, 754.
- [37] A. O. Patil, Y. Ikenoue, N. Basescu, N. Colaneri, J. Chen, F. Wudl, A. J. Heeger, *Synth. Met.* **1987**, *20*, 151.
- [38] Y. Ikenoue, Y. Saida, M. Kira, H. Tomozawa, H. Yashima, M. Kobayashi, *J. Chem. Soc. Chem. Commun.* **1990**, 1694.
- [39] A. O. Patil, Y. Ikenoue, F. Wudl, A. J. Heeger, *J. Am. Chem. Soc.* **1987**, *109*, 1858.
- [40] F. Tran-Van, M. Carrier, C. Chervot, *Synth. Met.* **2004**, *142*, 251.
- [41] S. L. Clark, M. F. Montague, P. T. Hammond, *Macromolecules* **1997**, *30*, 7237.
- [42] J. B. Schlenoff, S. T. Dubas, *Macromolecules* **2001**, *34*, 592.
- [43] S. T. Dubas, J. B. Schlenoff, *Macromolecules* **1999**, *32*, 8153.
- [44] N. G. Hoogeveen, M. A. Cohen Stuart, G. J. Fleer, M. R. Böhmer, *Langmuir* **1996**, *12*, 3675.
- [45] G. Decher, Y. Lvov, J. Schmitt, *Thin Solid Films* **1994**, *244*, 772.
- [46] J. Schmitt, T. Grunewald, G. Decher, P. S. Pershan, K. Kjaer, M. Losche, *Macromolecules* **1993**, *26*, 7058.
- [47] S. T. Dubas, J. B. Schlenoff, *Langmuir* **2001**, *17*, 7725.
- [48] W. K. Chan, P. K. Ng, X. Gong, S. J. Hou, *Appl. Phys. Lett.* **1999**, *75*, 3920.
- [49] L. S. M. Lam, W. K. Chan, *ChemPhysChem* **2001**, *2*, 252.
- [50] H. L. Wong, L. S. M. Lam, K. W. Cheng, K. Y. K. Man, W. K. Chan, C. Y. Kwong, A. B. Djurišić, *Appl. Phys. Lett.* **2004**, *84*, 2557.
- [51] A. Yakimov, S. R. Forrest, *Appl. Phys. Lett.* **2002**, *80*, 1667.
- [52] V. P. Singh, R. S. Singh, B. Parthasarathy, A. Aguilera, J. Anthony, M. Payne, *Appl. Phys. Lett.* **2005**, *86*, 082106.
- [53] The HOMO and LUMO levels of the polymer were estimated from the first oxidation and reduction potentials observed in the cyclic voltammogram, which were then compared with the oxidation potential of ferrocene internal standard.
- [54] Q. Qiao, J. T. McLeskey, *Appl. Phys. Lett.* **2005**, *86*, 153501.
- [55] Z. Liang, K. L. Dzienis, J. Xu, Q. Wang, *Adv. Funct. Mater.* **2006**, *16*, 542.
- [56] W. J. E. Beek, M. M. Wienk, R. A. J. Janssen, *Adv. Mater.* **2004**, *16*, 1009.
- [57] W. J. E. Beek, M. M. Wienk, M. Kemerink, X. Yang, R. A. J. Janssen, *J. Phys. Chem. B* **2005**, *109*, 9505.
- [58] E. Arici, N. S. Sariciftci, D. Meissner, *Adv. Funct. Mater.* **2003**, *13*, 165.
- [59] S. Conoci, D. M. Guldi, S. Nardis, R. Paolesse, K. Kordatos, M. Prato, G. Ricciardi, M. G. H. Vicente, I. Zilbermann, L. Valli, *Chem. Eur. J.* **2004**, *10*, 6523.
- [60] D. M. Guldi, F. Pellarini, M. Prato, C. Granito, L. Troisi, *Nano Lett.* **2002**, *2*, 965.
- [61] T. Piok, C. Brands, P. J. Neyman, A. Erlacher, C. Soman, M. A. Murray, R. Schroeder, W. Graupner, J. R. Hefflin, D. Marciu, A. Drake, M. B. Miller, H. Wang, H. Gibson, H. C. Dorn, G. Leising, M. Guzy, R. M. Davis, *Synth. Met.* **2001**, *116*, 343.
- [62] D. M. Guldi, I. Zilbermann, G. A. Anderson, K. Kordatos, M. Prato, R. Tafuro, L. Valli, *J. Mater. Chem.* **2004**, *14*, 303.
- [63] F. Ghebremichael, *Appl. Phys. Lett.* **2002**, *81*, 2971.
- [64] H. Mattoussi, M. F. Rubner, F. Zhou, J. Kumar, S. K. Tripathy, L. Y. Chiang, *Appl. Phys. Lett.* **2000**, *77*, 1540.
- [65] B. Pradhan, A. J. Pal, *Chem. Phys. Lett.* **2005**, *416*, 327.
- [66] J. Hjelm, R. W. Handel, A. Hagfeldt, E. C. Constable, C. E. Housecroft, R. J. Forster, *J. Phys. Chem. B* **2003**, *107*, 10431.
- [67] R. J. Forster, D. A. Walsh, N. Mano, F. Mao, A. Heller, *Langmuir* **2004**, *20*, 862.
- [68] R. J. Forster, D. Mulledy, D. A. Walsh, T. E. Keyes, *Phys. Chem. Chem. Phys.* **2004**, *6*, 3551.
- [69] T. Oekerman, T. Yoshida, C. Boeckler, J. Caro, H. Minoura, *J. Phys. Chem. B* **2005**, *109*, 12560.
- [70] B. C. O'Regan, S. Scully, A. C. Mayer, E. Palomares, *J. Phys. Chem. B* **2005**, *109*, 4616.

Received: June 15, 2006
Published online: October 2, 2006